The Unusually Slow Relaxation Kinetics of the Folding–unfolding of Pyrrolidone Carboxyl Peptidase from a Hyperthermophile, Pyrococcus furiosus

ARTICLE *in* JOURNAL OF MOLECULAR BIOLOGY · APRIL 2002

Impact Factor: 4.33 · DOI: 10.1006/jmbi.2001.5355 · Source: PubMed

3 AUTHORS:

Jai Kaushik
National Dairy Research Institute
58 PUBLICATIONS **800** CITATIONS
SEE PROFILE

Kyoko Ogasahara
Osaka University
108 PUBLICATIONS **2,433** CITATIONS
SEE PROFILE

Katsuhide Yutani
SPring-8
187 PUBLICATIONS **4,197** CITATIONS
SEE PROFILE

doi:10.1006/jmbi.2001.5355 available online at http://www.idealibrary.com on IDEAL® *J. Mol. Biol.* (2002) **316**, 991–1003

JMB

The Unusually Slow Relaxation Kinetics of the Folding-unfolding of Pyrrolidone Carboxyl Peptidase from a Hyperthermophile, *Pyrococcus furiosus*

Jai K. Kaushik[1,2], Kyoko Ogasahara[1] and Katsuhide Yutani[1]*

[1]*Institute for Protein Research Osaka University, 3-2 Yamada-oka, Suita, Osaka 565-0871 Japan*

[2]*Animal Biotechnology Centre National Dairy Research Institute, Karnal, 132001, India*

**Corresponding author*

In order to understand the thermodynamic and kinetic basis of the intrinsic stability of proteins from hyperthermophiles, the folding-unfolding reactions of cysteine-free pyrrolidone carboxyl peptidase (Cys142/188Ser) (PCP-0SH) from *Pyrococcus furiosus* were examined using circular dichroism (CD) and differential scanning colorimetry (DSC) at pH 2.3, where PCP-0SH exists in monomeric form. DSC showed a strong dependence of the shape and position of the unfolding profiles on the scan rate, suggesting the stability of PCP-0SH under kinetic control. On DSC timescales, even at a scan rate of 1 deg. C/hour, heat denaturation of PCP-0SH was non-equilibrium. However, over a long period of incubation of the heat-denatured PCP-0SH at pre-transition temperatures, it refolded completely, indicating reversibility with very slow relaxation kinetics. The rates of refolding of the heat-denatured PCP-0SH determined from the time-resolved DSC and CD spectroscopic progress curves were found to be similar within experimental error, confirming the mechanism of refolding to be a two-state process. The equilibrium established with a relaxation time of 5080 seconds (at $t_m = 46.5\,^{\circ}C$), which is unusually higher than the relaxation times observed for mesophilic and hyperthermophilic proteins. The long relaxation time may lead to the apparent irreversibility of an unfolding process occurring on the DSC experiment timescale. The refolding rate (9.8×10^{-5} s^{-1}) peaked near the t_m (=46.5 °C), whereas the stability profile reached maxima (11.8 kJ mol^{-1}) at 17 °C. The results clearly indicate the unusual mode of protein destabilization *via* a drastic decrease in the rate of folding at low pH and still maintaining a high activation energy barrier (284 kJ mol^{-1}) for unfolding, which provides an effective kinetic advantage to unusually stable proteins from hyperthermophiles.

Keywords: pyrrolidone carboxyl peptidase; hyperthermophile; differential scanning calorimetry; folding-unfolding kinetics; thermodynamic stability

Introduction

There have been tremendous efforts to understand the folding and stability of proteins. However, in spite of a large amount of data, the mechanism has not been deciphered clearly. Hyperthermophilic proteins have been investigated to elucidate the origin of enhanced stability and adaptation to very high temperatures. Proteins from hyperthermophiles maximally express bio-

Abbreviations used: PCP pyrrolidone carboxyl peptidase; PCP-0SH cysteine-free pyrrolidone carboxyl peptidase; DSC differential scanning calorimetry; t_m, the equilibrium unfolding temperature; T_d, the apparent unfolding temperature (at the peak of the DSC curve); T_c, temperature where $k_u = 1$; k_u, rate of unfolding; k_f, rate of refolding; k_r, rate of relaxation; τ_r, relaxation time; ΔH_c, calorimetric enthalpy of unfolding; ΔH_m, the enthalpy of unfolding at t_m; N, the native state; U, the unfolded state; T*, the transition state; E_u, the Arrhenius activation energy of unfolding; E_c, activation energy of unfolding at T_c; E_f, the activation energy of folding; C_P^{ex}, excess heat capacity; $\Delta C_P^{N\rightarrow U}$, the heat capacity of transition from the native (N) to the unfolded (U) state; $\Delta C_P^{N\rightarrow T^*}$, the heat capacity of N→T* transition; $\Delta C_P^{U\rightarrow T^*}$, the heat capacity of U→T* transition; ΔG, the Gibbs energy of stability.

E-mail address of the corresponding author: yutani@protein.osaka-u.ac.jp

0022-2836/02/040991–13 $35.00/0

logical functions under extreme conditions near 100 °C, and show unusually high denaturation temperatures.[1] It has been postulated that the extreme stability of these proteins is achieved through molecular adaptations to optimize factors such as hydrophobic effects, salt-bridges, hydrogen bonds, packing, and oligomerization, etc. A large number of protein structures determined at high resolution indicate that none of these factors distinctly accounts for the extraordinary stability of these proteins. Many of the hyperthermophilic proteins have been observed to achieve considerable kinetic stability under extreme conditions in the form of high activation energy and slow kinetics of unfolding,[2–5] resulting in a longer residence time for the protein molecules in the folded state under conditions that, thermodynamically, may not support the native state.

For hyperthermophile proteins, however, thermodynamic characterization has been hampered due to the propensity of these proteins to undergo irreversible thermal denaturation,[4–13] except for a few successful reports.[14–17] A considerable amount of data is now available on the unfolding kinetics, which indicates the propensity of hyperthermophilic proteins to undergo denaturation with a highly retarded rate constant limited by the high kinetic barrier. Interestingly, mesophilic protein ROP, a four-helix-bundle protein from *Escherichia coli*, also shows extremely slow relaxation kinetics of folding-unfolding,[18] and its loop deletion mutant has been shown to achieve hyperthermophilic stability[19] characterized by an extremely slow relaxation kinetics of folding in the transition zone.[20] On the other hand, hyperthermophilic CspB exhibited a retarded rate of unfolding but a conserved rate of refolding in comparison to the mesophilic homologues.[3] The folding data on these proteins have been obtained using chemical denaturants, whereas similar data on heat-denatured hyperthermophilic proteins is virtually non-existent.

The rate of refolding can be determined in an indirect way from the equilibrium and unfolding rate constants; however, it may lead to erroneous results due to the unavailability of experimental kinetic phases in the refolding reaction. This has limited our understanding of the mechanism of folding and the origin of stability of hyperthermophilic proteins. For a complete description of the stability profile and to understand the factors contributing to the extreme thermal stability of these proteins, it is important and a pre-requisite to obtain equilibrium thermodynamic and kinetic data under well-controlled conditions.

The present study is aimed at understanding the origin of the enhanced stability of proteins from hyperthermophiles in kinetic and thermodynamic terms. The pyrrolidone carboxyl peptidase (PCP) (E.C. 3.4.19.3) from a hyperthermophile, *Pyrococcus furiosus,* catalyses the cleavage of L-pyroglutamic acid from the N terminus of polypeptide chains.[21] PCP is a homotetramer constituted of subunits with 208 residues (22.8 kDa). PCP contains two cysteine residues per subunit, one in the active site (Cys142) and the other at the interface of the subunits (Cys188).[22] Cys188 partly forms an inter-subunit disulphide bond, resulting in the appearance of two peaks on the differential scanning calorimetry (DSC) curve.[23] On the other hand, cysteine-free PCP (PCP-0SH, C142/188S) has a single peak on the DSC curve, and its assembly form changes depending on the pH value. It exists as a tetramer in the region above pH 4.5, a dimer around pH 3.0, and a monomer below pH 2.7. PCP-0SH undergoes reversible unfolding in the dimeric form.[23] Therefore, it provides an excellent system to study the kinetics and thermodynamics of a hyperthermophilic protein in various states of oligomerization. Here, in order to understand the mechanism of intrinsic subunit stabilization of proteins from hyperthermophiles, we characterized the kinetics and thermodynamics of heat denaturation of the PCP-0SH monomer at pH 2.3 using DSC and circular dichroism (CD) measurements.

Results

The heat-denaturation of PCP-0SH at pH 2.3

Figure 1 shows the temperature-dependence of the partial molar heat capacity for PCP-0SH at pH 2.3 at various scan rates. The peak temperature of the DSC curves shifted considerably as a function of the scan rate. The DSC curves are asymmetrical and skewed toward the higher temperature side. These results indicate that the heat-denaturation of PCP-0SH did not attain equilibrium even at very slow scan rates and is under kinetic control. In the DSC of the cooling process after the first heating, no exotherm characteristic of the refolding process was observed even at a very slow scan rate (Figure 2). However, it was observed that the heat-denatured PCP-0SH could refold completely after incubation at 32 °C for 36 hours after the first heating (Figure 2).

The sedimentation equilibrium analyses of PCP-0SH at 4 °C immediately after heat-treatment and over complete refolding of the protein at 25 °C for one week gave apparent molecular masses of 25,800 and 21,200, respectively. These values are consistent with the molecular mass of 22,800 calculated for the monomer of PCP-0SH from the amino acid composition. The linearity of the log absorbance *versus* square of the radius curve suggested a homogeneous molecular distribution in the solution in both cases (Figures shown in Supplementary Material). These results confirmed that the heat-denatured PCP-0SH did not form aggregates and the protein exists in the monomer form at pH 2.3. These results indicate that the heat-denaturation of PCP-0SH at pH 2.3, where it exists as a monomer, is reversible, but that the rate of refolding is extremely slow. This means that DSC curves of PCP-0SH measured at very slow heating rates, where equilibrium is reached, can be treated in thermodynamic terms. However, the DSC

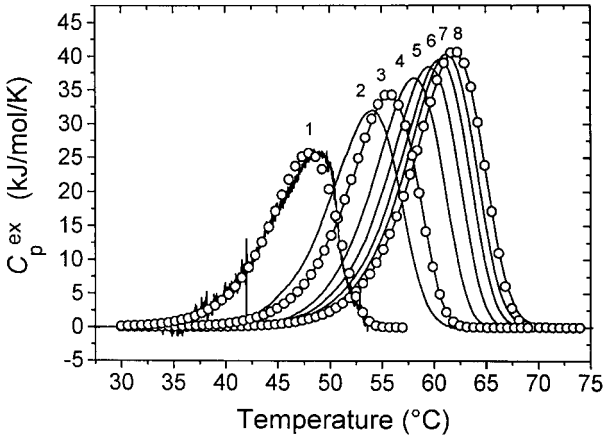

Figure 1. Dependence of excess heat capacity, C_p^{ex}, curves of PCP-0SH on scan rates. Samples at the same concentration (1.61 mg/ml) at pH 2.3 were measured at different scan rates. Curves 1 to 8 represent DSC curves at scan rates of 1, 9, 15, 30, 45, 60, 75, and 90 deg. C/hour, respectively. Open circles show the nonlinear least square fitting of the DSC curves to one-step irreversible model given by equation (12). For the sake of clarity only few representative fitting have been shown.

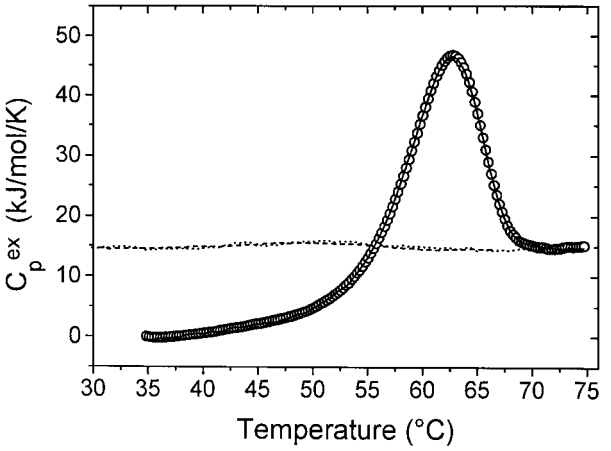

Figure 2. Reversibility of heat-denatured PCP-0SH at pH 2.3. Reheating (circles) of the sample was carried out after 36 hours incubation of the sample at 32 °C in the DSC cell itself after the first heating (continuous line). Both the heating were performed at a scan rate of 90 deg. C/hour. Dotted and dashed curves are excess heat capacity curves under a cooling mode at 9 and 30 deg. C/hour scan rates, respectively, after the first heating (90 deg. C/hour) to 75 °C.

measurement at extremely slow rates is not possible because of the limitations of the DSC machine. The denaturation process was non-equilibrium even at a highly diminished scan rate (1 deg. C/hour). Therefore, we analyzed the DSC curves obtained at different scan rates from the kinetic point of view.

Kinetic analysis of the unfolding DSC curves

We assumed that the heat denaturation of PCP-0SH at pH 2.3 was virtually reduced to a simple one-step irreversible process ($N \rightarrow U$), since the renaturation rate was extremely slow. According to the one-step irreversible process, the DSC curves can be expressed by equation (12) (Materials and Methods). The DSC curves at various scan rates fitted very well to the theoretical model described by equation (12) (Figure 1). The kinetic parameters obtained by analyzing the DSC curves are given in Table 1. Figure 3 shows the temperature-dependence of the enthalpy (ΔH_c) and the activation energy (E_u) of unfolding. The slope of the linear fit to the data provides the respective heat capacities of the processes. The heat capacity for the transition from the native state (N) to the transition state (T*) ($\Delta C_p^{N \rightarrow T^*}$) was very small (0.24 kJ mol^{-1} K^{-1}) and constituted only 2.6% of the total heat capacity of unfolding ($\Delta C_p^{N \rightarrow U} = 9.3$ kJ mol^{-1} K^{-1}). This suggests that the solvent exposure of the molecular surface in the transition state is quite similar to that in the native state (N), and that the heat capacity of unfolding, $\Delta C_p^{N \rightarrow U}$ is mainly related to the transition from the activated state to the unfolded state ($T^* \rightarrow U$). For a reversible two-state unfolding, the Arrhenius constants obey the relation:[5,24]

$$\Delta H = E_u - E_f \quad (1)$$

Table 1. Kinetic parameters of PCP-0SH unfolding at pH 2.3 determined by fitting the equation 12 to the excess heat capacity curves of unfolding obtained at various scan rates

Scan-rate (deg. C/hour)	E_u (kJ mol^{-1})	A	T_c (K)	T_d (K)	ΔH_c[a] (kJ mol^{-1})	k_u^b (s^{-1})
1	288.0	102.7	338.4	321.3	207.5	1.08×10^{-4}
9	279.1	99.8	337.6	327.5	276.5	1.18×10^{-3}
15	284.0	101.4	337.4	329.0	292.2	1.43×10^{-3}
30	288.5	103.0	337.4	331.4	315.1	2.82×10^{-3}
45	286.1	102.0	337.6	332.8	332.5	4.11×10^{-3}
60	285.1	101.6	337.7	333.8	344.3	5.38×10^{-3}
75	285.7	101.8	337.6	334.5	358.4	6.73×10^{-3}
90	286.6	102.1	337.8	335.2	356.8	7.94×10^{-3}

[a] Enthalpy of denaturation was evaluated by integrating the excess heat capacity curves.
[b] k_u was calculated with parameters given in this Table using equation (6).

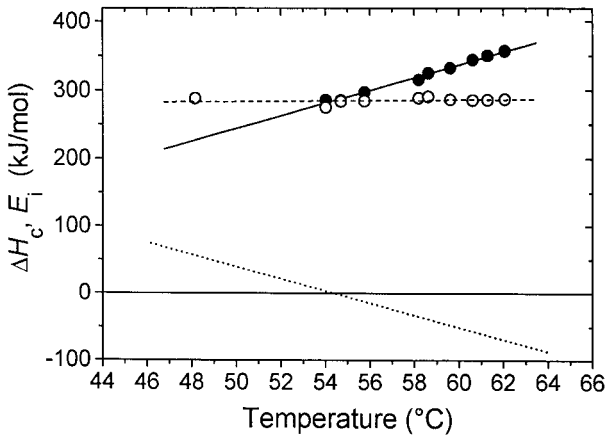

Figure 3. Temperature dependence of enthalpy (ΔH_c) and Arrhenius activation energy (E_u) of unfolding of PCP-0SH at pH 2.3. Solid and open circles represent the data of enthalpy and activation energy of unfolding, respectively. Continuous line is the linear fit ($\Delta H_c = -220.304(\pm 20.443) + 9.288(\pm 0.035) \times T$) to enthalpy data; the dashed line is the linear fit ($E_u = 271.56(\pm 20.42) + 0.237(\pm 0.351) \times T$) to the activation energy data and the dotted line represents temperature dependence of activation energy of refolding ($E_f = E_u - \Delta H_c$) ($E_f = 491.86 - 9.05 \times T$).

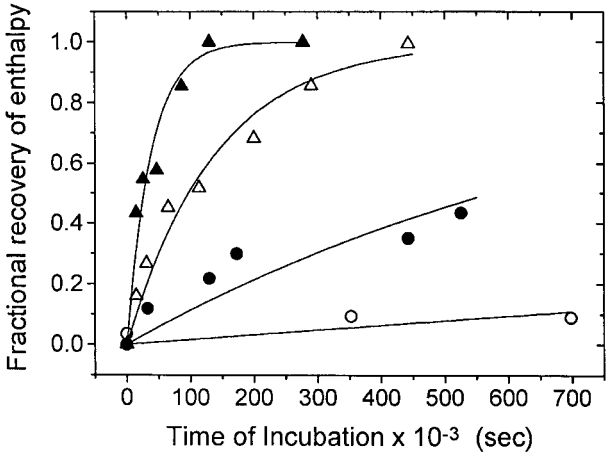

Figure 4. Recovery process of denaturation enthalpy of heat-denatured PCP-0SH at four different temperatures, 32 °C (▲), 25 °C (△), 18 °C (●), and 4 °C (○). Heat denaturation of the sample was carried out at 70 °C for ten minutes at pH 2.3. The solid lines indicate the single phase exponential fits (equation (14)).

from which E_f, the activation energy of refolding, can be determined at any temperature. The dependence of E_f on temperature was observed to be linear with a slope corresponding to the heat capacity of activation for refolding, $\Delta C_p^{U \rightarrow T^*}$, to be −9.05 kJ mol^{-1} K^{-1} (Figure 3).

Refolding of the heat-denatured PCP-0SH

Time resolved DSC

DSC was employed to determine the refolding rate by measuring the progress of recovery of ΔH as a function of time from the heat-denatured state. DSC curves of PCP-0SH at pH 2.3 were measured after incubation of the heat-denatured samples for various times at several temperatures. Figure 4 shows the progress curves of the recovery in the enthalpy of unfolding, which is proportional to the population of the native-state species. The progress curves at 25 and 32 °C finally reached the value of enthalpy corresponding to that of an intact sample. This indicates that the heat-denatured PCP-0SH has recovered completely, although this takes a long time. The observed rate of refolding, $k_{f,\,obs}^{DSC}$ (Table 2), was obtained by assuming the progress curves to be a single-exponential phase (equation (14)). Using DSC, it was not possible to resolve the fast phase, if any, preceding the slow phase. Nonetheless, data at low temperatures indicate that there might not be any fast phase, because the enthalpy of unfolding was almost linear as a function of time and the first exponential phase itself seemed like a linear phase at low temperatures. Even if any fast phase existed, it should have been unstructured with negligible enthalpy. The small number of data obtained by this method did not

Table 2. The observed rate constants of refolding of heat denatured PCP-0SH determined by DSC and CD at various temperatures

		$k_{f,\,obs}^{CD}$ (s^{-1})	
Temperature (°C)	$k_{f,\,obs}^{DSC}$ (s^{-1})	At 220 nm	At 280 nm
18	1.2×10^{-6}		
20		8.79×10^{-6}	2.98×10^{-6}
25	7.17×10^{-6}		
28		2.54×10^{-5}	
32	2.62×10^{-5}	5.07×10^{-5}	3.89×10^{-5}
37		9.77×10^{-5}	7.76×10^{-5}
		8.77×10^{-5}[a]	
40		9.98×10^{-5}	8.13×10^{-5}
44			1.29×10^{-4}

[a] PCP-0SH in freshly prepared urea (5.5 M), pH 2.3 was incubated at 48 °C for 30 minutes followed by overnight incubation at 37 °C before the refolding experiment, which was initiated by transferring the urea-denatured protein solution (27.5-fold dilution) to 20 mM Gly-HCl buffer (pH 2.3 at 37 °C).

provide a high-resolution window to observe the intermediate steps; nevertheless, this clearly indicates that structure formation or nucleus propagation to form the native structure is extremely slow.

Time-resolved CD spectroscopy

Figure 5(a) and (b) show the refolding progress curves of the heat-denatured PCP-0SH monitored by changes in CD values at 220 and 280 nm, indicating the formation of secondary and tertiary structures, respectively, at different temperatures. The measurements had a dead time of approximately two to four minutes, which is not very long in comparison to the total time taken by complete refolding. In comparison to protein folding on a millisecond to seconds timescale, this dead time is equivalent to only sub-milliseconds to milliseconds. Secondly, this time includes the time required for equilibration with the cuvette temperature. Thirdly, the initial amplitude for all the experiments at various temperatures was similar within experimental noise, and the progress curve at 20 °C was an exponential curve stretched almost like a linear curve, suggesting the absence of a burst phase, which might not have been detected due to the comparatively large dead time. Therefore, the time progress curves were fitted to a single-exponential phase to determine the observed rate of refolding, $k_{f,obs}^{CD}$ (Table 2). The data in Table 2 indicate an extremely slow rate of refolding of heat-denatured PCP-0SH. The refolding initiated by diluting the urea-denatured PCP-0SH at 37 °C showed a rate of relaxation (Table 2) similar to that observed for heat-denatured protein at 37 °C.

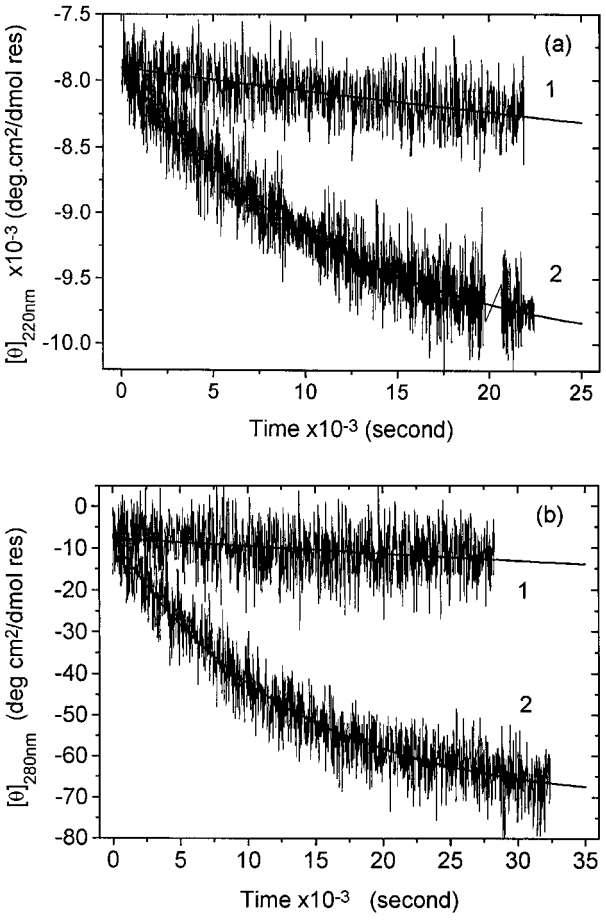

Figure 5. Temperature dependence of refolding of PCP-0SH measured at pH 2.3 by changes in CD at (a) 220 nm, and (b) 280 nm as a function of time. For clarity, only curves at temperatures 20 °C (curve 1) and 37 °C (curve 2) have been depicted to show the trend. The continuous lines indicate the single phase exponential fits (equation (14)).

Determination of the equilibrium unfolding temperature (t_m)

It was revealed that the heat-denaturation of monomer PCP-0SH was reversible. Although the equilibrium heat-denaturation curve of monomer PCP-0SH at pH 2.3 could not be obtained by DSC due to the extremely slow relaxation kinetics, the fraction of the refolded form at various temperatures could be estimated from the ΔH value obtained for the second DSC curve of the heat-denatured PCP-0SH incubated for a sufficiently long time at various temperatures to reach equilibrium. Figure 6 shows the fraction of refolding ($\Delta H_2/\Delta H_1$) *versus* temperature of incubation after the first heating (see Materials and Methods), where ΔH_1 and ΔH_2 are the enthalpy changes during the first heating and the reheating, respectively. The ratio $\Delta H_2/\Delta H_1$ corresponds to the fraction of the refolded form at each temperature, whereas the curve in Figure 6 corresponds to the equilibrium denaturation transition. The curve obtained was highly cooperative.

The non-linear least-squares fitting of curve ($\Delta H_2/\Delta H_1$ *versus* temperature) to equation (13) provided the values of the temperature midpoint (t_m) and the enthalpy of unfolding (ΔH_m) to be 46.8(±1) °C and 295(±71) kJ mol^{-1}, respectively, assuming $\Delta C_p = 9.3$ kJ mol^{-1} K^{-1} obtained by DSC (Figure 3). On the other hand, using the scan rate-dependent DSC, the peak temperature was 48.1 °C at a scan rate of 1 deg. C/hour (Table 1) indicating that unfolding of PCP-0SH could not reach equilibrium even at the slowest possible scan rate.

Discussion

Apparent irreversibility of heat-denatured PCP-0SH

PCP-0SH at pH 2.3 apparently did not reach equilibrium unfolding at all practical scanning rates available on the commercial calorimeters; also, it did not refold even at a very slow rate of cooling in the DSC experiment. However, refolding experiments indicate that heat-denatured PCP-0SH could recover completely after a long period of incubation at pre-transition temperatures,

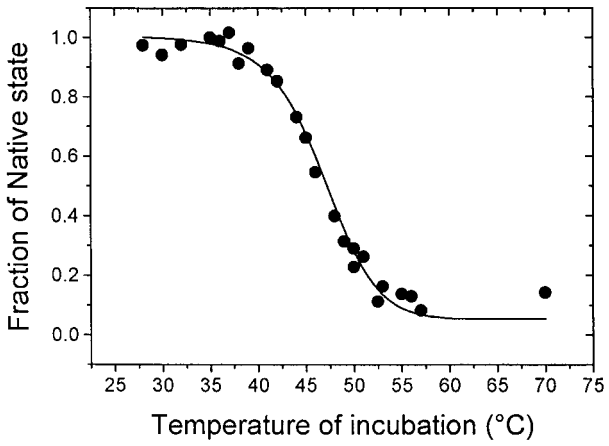

Figure 6. Fraction of refolding of PCP-0SH in the equilibrium state after long incubation of the heat-denatured sample at various temperatures. The fractions were obtained from the ratio, ΔH_2 (second heating)/ ΔH_1 (first heating) (see Materials and Methods). The fitting (continuous line) of equation (13) to data gave $\Delta H_m = 295(\pm 71)$ kJ mol^{-1} and $t_m = 46.8(\pm 1)$ °C assuming $\Delta C_p = 9.3$ kJ mol^{-1} K^{-1} from the calorimetric data.

suggesting that the folding of PCP-0SH is accompanied by extremely slow relaxation kinetics. The sedimentation analysis of heat-denatured and completely refolded PCP-0SH indicated clearly that it remains in the monomeric form and does not form aggregates over heating, precluding the possibility of slow refolding due to aggregation. Heat-denatured PCP-0SH remains in the unfolded state over the period of sedimentation of 24 hours at 4 °C, as suggested by negligible refolding measured by DSC (Figure 4). The similar folding rate constants observed for urea and heat-denatured PCP-0SH clearly indicate the inherent slowness of PCP-0SH folding at low pH values.

Computer simulation[24,25] has shown that even a completely reversible process may behave like an irreversible process at high heating rates. Lepock *et al.*[24] have estimated that, for a thermal transition to be in equilibrium, the ratio of the scan rate to the rate constant (v/k_i) should not exceed 0.1 and the process should be completely irreversible at $v/k_i \geqslant 10$. The value of v/k_i for PCP-0SH at t_m (46.5 °C) was estimated to be 2.21 (at the slowest v =1 deg. C/hour), which is considerably higher than the requirement of the process to be in equilibrium. This clearly shows that, in spite of the reversibility of the unfolding process, it cannot reach equilibrium on the DSC timescale, because both the unfolding as well as the refolding are extremely slow in the transition zone ($k_u = k_f$ at t_m) in comparison to the available scan rates. Therefore, despite 100 % reversibility, PCP-0SH may not undergo equilibrium unfolding even at an extremely slow rate of heating (1 deg. C/hour) due to the unusually long relaxation time (5080 seconds at $t_m = 46.5$ °C). These observations strongly support the interesting proposal based on computer simulations by Potekhin & Kovrigin,[25] that even the simplest two-state reversible transition can behave irreversibly when an unfavorable combination of cooling rate, relaxation time, and activation energy of refolding occurs. Therefore, as opposed to the real irreversibility due to alteration of the polypeptide chain, the experimental instances of irreversibility might be caused by the slow establishing of the folding-unfolding equilibrium due to the kinetic trapping of the unfolded state. An analogous situation is encountered in the form of a hysteresis between unfolding and refolding reactions mediated by GuHCl when relaxation kinetics is extraordinarily slow.[20]

To our knowledge, almost no data exist on the refolding kinetics of heat-denatured hyperthermophilic proteins to allow a direct comparison; however, a few reports exist on the refolding of chemical denaturant-mediated denatured proteins. The refolding of GuHCl-denatured PCP-0SH at 25 °C and pH 7 occurs with a relaxation time of about ten seconds,[26] whereas cold-shock protein CspB from *Thermotoga maritima* refolds on a millisecond timescale[3] at 25 °C and pH 7. A myriad of proteins reported to undergo two-state kinetics exhibit a large dynamic range of folding rates over a 10^6-fold difference between the fastest and the slowest-folding proteins.[27] The relaxation kinetics for a large number of well-studied small mesophilic proteins has been observed at milliseconds to seconds timescales.[27,28] Based on fast-folding proteins Plaza del Pino *et al.*[28] contend that there cannot be too slow establishment of the protein folding-unfolding equilibrium that may result in the experimental instances of irreversibility. On the other hand, our experimental data clearly support the computer simulation result obtained by Potekhin & Kovrigin,[25] which indicated the possibility of the kinetic trapping of the unfolded state leading to the apparent irreversibility on the DSC timescale. Most of the proteins reported earlier have shown much higher folding rates than that of PCP-0SH at pH 7,[26] where it folds faster than at pH 2.3. The mesophilic Rop protein has been shown to undergo exceedingly slow refolding kinetics at 19 °C with a relaxation time of 97 hours at the midpoint of transition induced by GuHCl.[18]

The rates of unfolding-refolding reactions and the thermodynamic stability of PCP-0SH

The heat-denaturion of PCP-0SH was completely reversible at pH 2.3, although the unfolding-refolding reactions were characterized by extremely slow kinetics. The rate of relaxation of PCP-0SH, k_r, is determined mainly by k_u at higher temperatures as, shown in Figure 7(a); however, in the transition zone or at lower temperatures k_u becomes very small and k_r is not compensated by k_f as temperature decreases, unlike in the case of other studied proteins,[3,27,28] because k_f also decreased at lower temperatures below t_m (Figure 7(a)). The rate of refolding reached maxima near the t_m value and

decreased on both sides of it. The relaxation time ($\tau_r = k_r^{-1}$) evaluated at t_m (46.5 °C) was 5080 seconds. Using the forward and reverse rate constants, k_u and k_f, respectively, the equilibrium constant K was evaluated to determine the stability profile (ΔG *versus* temperature) of PCP-0SH at pH 2.3 (Figure 7(b)). A fitting of the obtained stability data to the modified Gibbs-Helmholtz equation:

$$\Delta G(T) = \Delta H_m(1 - T/T_m) - \Delta C_p(T_m - T + T\ln(T/T_m)) \quad (2)$$

where $\Delta G(T)$ is the Gibbs energy at any temperature T, yielded the temperature of unfolding (t_m), the enthalpy of unfolding (ΔH_m) and the heat capacity (ΔC_p) to be 46(±1.2) °C, 278(±40) kJ mol^{-1}, and 9.15(±3.08) kJ mol^{-1} K^{-1}, respectively. These values were in good agreement with those obtained independently by equilibrium refolding study (see the legend to Figure 6). The stability curves produced by two independent methods are almost superimposed (Figure 7(b)).

A drastic decrease in the unfolding rate has been generally cited as the main mechanism of kinetic and thermodynamic stabilization of hyperstable proteins,[3,4,12,26,29] because folding rates remain conserved and essentially independent of the stability of the native state for a two-state process;[3,29,30] conversely, an increase in the unfolding rate accounts for a decrease in the thermodynamic stability of a protein. However, our results do not fully support this generalization. We observed a considerably slow unfolding rate (~10^{-7} s^{-1} at 25 °C) even at very low pH values, where mesophilic PCP is completely unfolded. However, it was also accompanied by an extremely slow rate of refolding (~10^{-5} s^{-1} at 25 °C) resulting in a very small Gibbs energy of stabilization, 11.8 kJ mol^{-1} at 25 °C (Figure 7(b)). Previously, Ogasahara *et al.*[26] have reported the k_f and k_u values of PCP-0SH to be ~0.1 s^{-1} and 1.7 × 10^{-14} s^{-1}, respectively, resulting in high thermodynamic stability of PCP-0SH at 25 °C and pH 7 ($\Delta G = 78$ kJ mol^{-1}). In the present study at pH 2.3, the values of both k_f and k_u seem to be shifted in an opposite manner, with an increase in k_u and a decrease in k_f compared with those at pH 7. On changing the pH from 7 to 2.3, the refolding rate decreased by a factor of ~10^4. It indicates that the thermodynamic stability may be controlling the relaxation kinetics of folding of PCP-0SH. Several other reports[27,31–34] indicate the decisive role of stability in the folding of proteins. However, a drastic effect of stability on the folding kinetics as observed for hyperthermophilic PCP-0SH has not been observed earlier (see Plaxco *et al.*[34]).

The specific heat capacity of unfolding for PCP-0SH was observed to be 44.7 J (mol residue)$^{-1}$ K^{-1}. However, it was estimated to be 76 J (mol residue)$^{-1}$ K^{-1} based on the change in the total accessible surface area (=19,532 Å^2)[22] over complete unfolding by using the equation of Myers *et al.*[35] based on a 45 protein database corrected for the disulfide bonds. The observed heat capacity of unfolding was significantly lower than the calculated heat capacity. The compact states due to

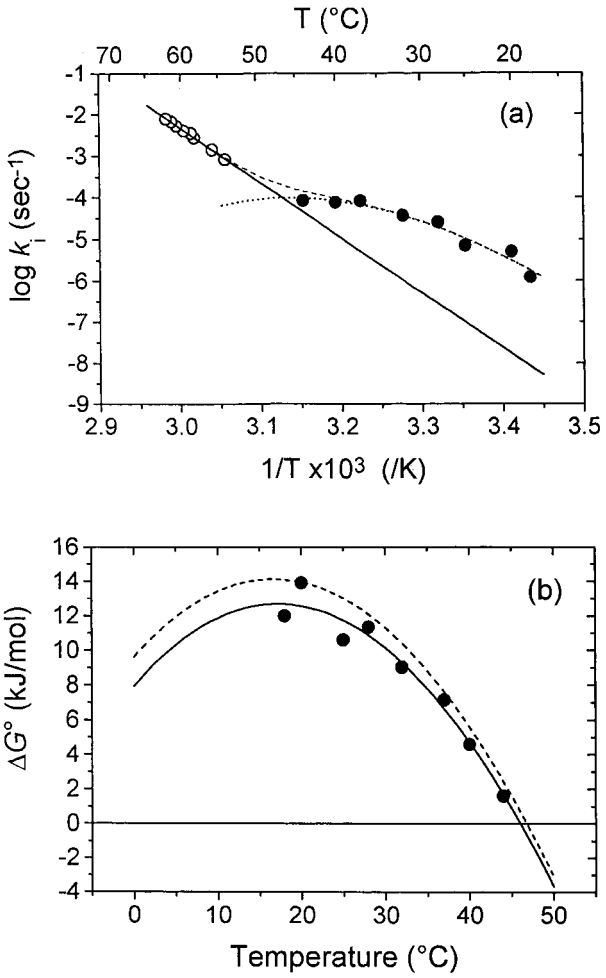

Figure 7. Temperature dependence of kinetic and thermodynamic parameters of PCP-0SH at pH 2.3. (a) Temperature dependence of the logarithms of unfolding (k_u), refolding (k_f), and relaxation ($k_r = k_u + k_f$) rate constants. The log k_u values at lower temperatures (continuous line) were extrapolated by fitting the k_u (open circles: data of Table 1) to the Arrhenius equation (equation (6)), and assuming E_u a function of temperature ($E_u = E_c + \Delta C_p^{N \to T^*}(T - T_c)$) and using the $\Delta C_p^{N \to T^*}$ value of 0.24 kJ mol^{-1} K^{-1}. Broken line represents k_r values, which were obtained by the summation of k_u values above and k_f values observed at the corresponding temperatures determined from the DSC, near and far UV-CD time progress curves (Table 2). For clarity, the refolding data, solid circles, have been shown as an average obtained by several techniques at a given temperature. The dotted fitted curve to log k_f is only empirical. (b) Solid circles represent the unfolding Gibbs energies obtained from the equilibrium constant ($K = k_u/k_f$). The continuous line is the stability curve fitted to the data points using equation (2), whereas the broken line is that generated (using equation (2)) from the thermodynamic parameters given in legend of Figure 6.

cross-links show a comparatively smaller change in the accessible surface area with unfolding.[35,36] The small heat capacity for PCP-0SH could result from the incomplete exposure of the hydrophobic groups in the unfolded state. The heat-denatured PCP-0SH contained significant helical structure and seems considerably structured as evident from the large ellipticity at 220 nm (Figure 5(a)). However, the heat-denatured state was enthalpically equivalent to the completely unfolded state, because no endotherm was observed during heating the heat-denatured PCP-0SH immediately after heat treatment. In addition, all the aromatic groups buried inside PCP-0SH were exposed in the heat-denatured state, as was evident from the complete loss of the negative ellipticity at 280 nm (Figure 5(b)). The heat-denatured proteins have been known to be comparatively more compact than the GuHCl or urea-denatured proteins; however, thermodynamically, these unfolded states may not differ much.[37]

Thermophilic proteins have been known to achieve stability at higher temperatures by shifting the stability maxima to a higher temperature, raising, and/or flattening the stability curve over a broad temperature range. The high stability may be achieved *via* one of the above mechanisms or by their combination.[17,29,38,39] The flattening of the stability curve, which can be achieved by decreasing the heat capacity of unfolding, has been employed by several hyperthermophilic proteins.[16,17,40] It seems that PCP-0SH may be reflecting the same trend to achieve stability over a broad temperature range. The specific heat capacity of the unfolding of PCP-0SH is very close to 40.6 J (mol residue)$^{-1}$ K^{-1} observed for a small DNA-binding protein, Sso7d, and domain II of glutamate dehydrogenase from *Sulfolobus solfataricus*[16] and *Thermotoga maritima*,[17] respectively. Therefore, it seems that the observed low heat capacity of unfolding may be an inherent property of PCP-0SH for achieving thermodynamic stability over a broad range of temperature.

In the studies on the dependence of protein stability on the denatured-state structure, Sugita & Kitao[41] have reported that calculated $\Delta\Delta G$ values for mutant proteins are in good agreement with the experimental $\Delta\Delta G$ values when a native-like structure is employed; whereas in the other models (extended and random-coil like conformations) the calculated value differs sharply from the experimental one. These results suggest that the stability of PCP-0SH might increase due to decrease in the entropy of the denatured state because the lower specific heat capacity of unfolding for PCP-0SH means that the conformation of the protein in the denatured state is not an extended form but a partly folded one. Recently, based on calorimetry and X-ray structural studies, the tryptophan synthase α subunit from *P. furiosus* has been reported to be stabilized by entropic effects compared with a homologous protein from a mesophile.[42]

Structural basis of slow kinetics

It is important to investigate the possible structural features responsible for the unusually slow relaxation kinetics of PCP-0SH at low pH. Recently, the crystal structure of PCP-0SH has been solved by X-ray analysis, which indicates that, in spite of the similar number of ion pairs per residue as observed in the mesophile homologue from *Bacillus amyloliquefaciens* (BaPCP), the networks of ion pairs at the subunit interfaces may contribute to the higher stability of the tetramer of PCP-0SH.[22] Electrostatic interactions have been suggested to play an important role in the slow unfolding kinetics of hyperthermophilic proteins.[3,4,12,29,43] However, the present results at pH 2.3, where PCP-0SH exists in the monomeric form devoid of all the inter-subunit electrostatic interactions, do not seem to support the role of surface electrostatic interactions in slow unfolding. Hyperthermophilic rubredoxin from *P. furiosus* studied at pH 2.0 also shows a significantly retarded unfolding rate,[4] which accounts for its high level of stability in comparison to the mesophilic rubredoxin at pH values where electrostatic interactions do not exist. In addition, the monomer form of PCP-0SH has two pairs of buried ion pairs (between Arg73 and Glu79, and Lys177 and Glu14); however, such ion pairs have been shown to incur a large solvation penalty and contribute negligibly towards the thermodynamic stability of proteins.[44–46] Therefore, it appears that the high kinetic stability of PCP-0SH could reside in the structural elements composing the three-dimensional conformation other than electrostatic interactions.

Several reports have suggested the increased occurrence of proline in thermophilic proteins.[47–50] The PCP-0SH subunit contains 16 proline residues that constitute approximately 7.7% of the sequence,[22] which is not remarkably higher than that in mesophilic homologues, BaPCP (7%) and PCP from *B. subtilis* (7.4%), although this is significantly higher than the average occurrence of 4.2% in mesophilic as well as some thermophilic proteins.[51] Tanaka *et al*.[22] have suggested that proline might not be a factor responsible for the higher stability of PCP from hyperthermophiles.

The *cis-trans* isomerization of proline is a slow process responsible for the rate-limiting step in the protein folding. In PCP-0SH, out of the 16 proline residues, Pro159 is present in the *cis* form in the folded state. However, the rate of refolding of PCP-0SH is too slow to be explained by the *trans* → *cis* isomerization step. The *cis-trans* isomerization, which takes place at hundreds of seconds,[52] may contribute to the slow process, but it should not be the rate-limiting step in the present case.

Transition state structure

The heat capacity has been observed to be directly proportional to the change in accessible surface area of proteins upon folding or unfolding.[35] In an unfolding reaction, the

$\Delta C_p^{N \to T^*}$ should therefore give a measure of exposure of buried groups upon formation of the transition state. Thus, the fractional solvent exposure of the transition state relative to the denatured state can be estimated from $\Delta C_p^{N \to T^*}/\Delta C_p^{N \to U}$, where $\Delta C_p^{N \to U}$ is the heat capacity of denaturation. This quantity for PCP-0SH is only 0.026; i.e. the change in solvent-accessible surface area upon formation of the transition state is below 3% of that upon denaturation, suggesting that the transition state of PCP-0SH is as compact as the native state. In a two-state kinetics, the formation of the transition state should be accompanied by similar compactness in the refolding process. The relative compactness of the transition state of PCP-0SH is considerably higher than observed for many other proteins,[27] indicating that the formation of the transition state in slow folding proteins takes place late in the folding process. This is consistent with data on fast-folding proteins wherein the transition state has relatively larger solvent exposure.[53]

The structure of the native PCP-0SH does not provide distinct clues responsible for the slow folding rate. However, the formation of two ion pairs (Arg73-Glu79 and Lys177-Glu14), which have to be buried inside, might be limited due to very low pH. The formation of these ion pairs should be preceded by a chain compaction step to provide a low dielectric constant environment required for the formation of ion pairs at low pH. This means that the formation of salt-bridges should be a late event coinciding with the formation of the transition state and could be responsible for the rate-limiting step in the folding process. At present, we do not have experimental support for this mechanism, which needs to be investigated by replacing these ion pairs.

Biological significance

In addition to thermodynamic stability, many proteins are equipped with kinetic stability for an extended half-life against the *in vivo* irreversible processes.[28] These kinetic processes become more important at extremes of environmental conditions; like high salinity, low or high pH, high pressure, and/or high temperatures, etc.; and exert extra evolutionary pressure on organisms to impart considerable thermodynamic as well as kinetic stability on proteins. Our results on the hyperthermophilic protein PCP-0SH indicate the importance of kinetic stability at conditions where the mesophilic BaPCP unfolds completely.[26] PCP-0SH possesses low thermodynamic stability (11.8 kJ mol^{-1}) but considerably high kinetic stability (284 kJ mol^{-1}) at pH 2.3. The present results, though obtained far away from physiological conditions for *P. furiosus*, point towards the evolutionary strategy adopted by hyperthermophiles to survive at high temperatures where irreversible processes become very important. Plaza del Pino *et al*.[28] have suggested an extreme case where proteins can achieve the native state solely on the basis of kinetic stability when unfolding Gibbs energy is negative under certain non-physiological conditions. PCP-0SH existing in monomeric native state in spite of having marginal thermodynamic stability seems to be near to such an extreme case. However, at low pH, the small thermodynamic stability (large value of K_{eq}) and slow rate of unfolding (small k_u) also results in the rate of refolding to be slow also ($k_f = k_u/K_{eq}$), which may not be biologically relevant. Hyperthermophiles growing at high temperatures may have an evolutionary pressure to select proteins with exceedingly reduced rates of unfolding rather than very high folding rates, because the rate of irreversible modification of proteins depends upon the rate of unfolding.[28]

Small proteins folding *via* a two-state process show a wide variation in folding rates, from microseconds[33,54] to seconds.[55] This range is further extended by larger proteins folding *via* complex multi-state kinetics; e.g. C-terminal domain from PGK[56] folds $\sim 10^6$ times more slowly than the fastest-folding proteins, a G46A/G48A mutant of λ repressor[33] and the B-domain of staphylococcal protein A.[54] PCP-0SH at pH 2.3 seems to be the slowest-folding protein, which further widens the existing range of protein folding rates.

Conclusion

The thermal unfolding of pyrrolidone carboxyl peptidase (Cys142/188Ser) from a hyperthermophile was completely reversible at pH 2.3 where it is in a monomer form. Therefore, the unfolding-refolding reactions could be kinetically and thermodynamically analyzed. The rate constants of both unfolding and refolding were extremely slow. The rate constant of folding reached maxima ($k_f = 9.8 \times 10^{-5}$ s^{-1}) near the t_m value (46.5 °C) and decreased on both sides of it. The relaxation time ($\tau_r = k_r^{-1}$) evaluated at t_m was 5×10^3 seconds. The kinetic stability of this thermophile protein is caused by a considerably slow unfolding rate. The unusually slow rate of refolding seems to be determined by the small thermodynamic stability of PCP-0SH at low pH.

Materials and Methods

PCP-0SH (C142/188S) cloned in *E. coli* was expressed and purified from a 5×3 l culture as described.[23] The protein was purified to a level of homogeneity as determined by SDS-PAGE. The protein solution was dialyzed exhaustively for 24 hours at 4 °C against 20 mM glycine-HCl buffer (pH 2.3), followed by filtering through a 0.22 μM pore size disposable filter assembly in a similar way for all sets of experiments. The protein concentration was determined using the absorption coefficient of 0.66 $(mg/ml)^{-1}$ at 278 nm with a cell of 1 cm light-path length.[26] Urea (specially prepared reagent grade)

from Nacalai Tesque (Kyoto, Japan) was used without further purification. Other chemical reagents used were of analytical grade.

Differential scanning calorimetry (DSC)

Calorimetric data were recorded on a high-sensitivity VP-DSC, controlled by VPViewer™ software package (Microcal Inc., USA), with a cell volume of 0.51 and at an excess pressure of 30 psi (1 psi ≈ 6.9 kPa) to avoid degassing during heating. The DSC cells were filled with the last dialysis buffer, and several baselines were collected until they became superimposed, by running the calorimeter overnight. The buffer and PCP-0SH samples were degassed by evacuation before loading into the DSC cells. The pH of the sample was always measured at room temperature before and after the heating.

Scan rate-dependent DSC

Experiments at different heating rates (1, 9, 15, 30, 45, 60, 75 and 90 deg. C/hour) were carried out at a protein concentration of 1.61 mg/ml. The excess heat capacity curves for the protein were corrected by subtracting the corresponding buffer baseline recorded at the same scan rate and then normalized by protein concentration to estimate the enthalpy and heat capacity of unfolding using the Origin™ software package (OriginLab, USA).

Analysis of excess heat capacity curves

The excess heat capacity curves at various scan rates were analyzed using the kinetic scheme as follows. The kinetic scheme for the reversible equation:

$$\mathrm{N} \underset{k_f}{\overset{k_u}{\rightleftharpoons}} \mathrm{U}$$

where N is the native state species, U is the reversibly unfolded species, k_u is the rate constant for unfolding and k_f, the rate constant for refolding, can be described by the differential equations:

$$\mathrm{dN}/\mathrm{d}t = -k_u\mathrm{N} + k_f\mathrm{U} \tag{3}$$

$$\mathrm{dU}/\mathrm{d}t = k_u\mathrm{N} - k_f\mathrm{U} \tag{4}$$

However, for an irreversible or apparently irreversible one-step process (N → U), the above expressions reduce to:

$$\mathrm{dN}/\mathrm{d}t = -k_u\mathrm{N}$$

$$\mathrm{dU}/\mathrm{d}t = k_u\mathrm{N}$$

The rate of change in fractional concentration of the unfolded species (F_U) can be written as follows:

$$\mathrm{d}F_U(t)/\mathrm{d}t = k_u(T)[1 - F_U(t)] \tag{5}$$

where the fractional concentration of the native species $F_N = 1 - F_U$, and t is the time. The temperature-dependence of the unfolding process can be approximated by the Arrhenius relation:

$$k_u(T) = \mathrm{e}^{(A - E_u/RT)} \tag{6}$$

where E_u is the activation energy for the (N → U) process, A is a constant containing the entropy of activation, R is the universal gas constant, and T is absolute temperature. However, in a temperature-scanning process where T changes linearly with time, the function $\mathrm{d}F_U[T(t)]$ can be obtained by substituting k_u from equation (6) into equation (5), and T with $T_o + \nu t$, where T_o is the starting temperature and ν the scan rate, as follows:

$$\mathrm{d}F_U[T(t)]/\mathrm{d}t = \mathrm{e}^{(A - E_u/R(T_o + \nu t))}(1 - F_U[T(t)]) \tag{7}$$

In the present case, the total enthalpy change is related to the N → U step; therefore, the excess heat capacity, $C_p^{ex}(T)$ of the process is directly proportional to the rate of disappearance of the native species as a function of temperature:

$$C_p^{ex}(T) \propto [-(\mathrm{d}F_N/\mathrm{d}T) = (\mathrm{d}F_U/\mathrm{d}T)]$$

or:

$$C_p^{ex}(T) = \Delta H_c(\mathrm{d}F_U/\mathrm{d}T) = (\Delta H_c/\nu)k_u(T)[1 - F_U(T)] \tag{8}$$

where ∝ is the proportionality constant, and ΔH_c is the calorimetric enthalpy. To simplify the procedure for determining C_p^{ex}, approximations described by Fujita *et al.*[57] were used to obtain the analytical solution for $\mathrm{d}F_U[T(t)]$ in equation (7):

$$\mathrm{d}F_U[T(t)] = 1 - \exp\{-(RT_c^2/E_u\nu)\exp[E_u(T - T_c)/RT_c^2]\} \tag{9}$$

where T_c is the temperature at which $k_u = 1$ and can be written as $T_c = T(t) - \nu(t - t_o)$, where $t = t_o$ at T_c so that $T_c = E_u/AR$. The Arrhenius relation will take the form:

$$k_u(T) = \exp[A - E_u/R(T_c + \nu(t - t_o))] \tag{10}$$

for $\nu(t - t_o) \ll T_c$, the $(t - t_o)$ term can be expanded in a Taylor series wherein higher-order terms can be neglected,[58] giving:

$$k_u(T) = \exp(A - E_u/RT_c^2) \tag{11}$$

Substituting the values of $\mathrm{d}F_U[T(t)]$ and $k_u(T)$ from equations (9) and (11), respectively, into equation (8) gives:

$$C_p^{ex}(T) = (\Delta H/\nu)\exp(A - E_u/RT)\exp\{-RT_c^2/(E_u\nu) \times [\exp(E_u(T - T_c)/(RT_c^2))]\} \tag{12}$$

Using the non-linear least-squares fitter employing the Levenberg-Marquardt algorithm as provided in the Mathematica™ software package (Wolfram Research Inc.), equation (12) was fitted to the excess heat capacity curves (C_p^{ex} *versus* T) to evaluate the values of kinetic parameters, E_u, A and T_c, by freely floating them simultaneously. The scan rate, ν (K/minute) and the value of ΔH_c determined by integrating the excess heat capacity curves were supplied as fixed parameters. The kinetic parameters obtained by floating them free simultaneously while fitting a DSC curve are not independent, and error in one is transmitted to the other two in a compensatory manner, because the ratio E_u/T_cA is a constant equal to R.

Analytical ultracentrifugation

Sedimentation experiments were performed in a Beckman Optima XL-A analytical ultracentrifuge using the

Kel-F cell (cell length 12 mm) and An-60 Ti rotor at a speed of 22,000 rpm. PCP-0SH dialyzed overnight at 4 °C against 20 mM Gly-HCl buffer (pH 2.3), was heat-denatured at 62-64 °C for 14 minutes and cooled immediately by incubating on ice. The heat-denatured protein sample was divided into two lots. The first part was used immediately to load the ultracentrifuge cell pre-cooled to 4 °C. The second part was incubated for refolding at 25 °C for one week before sedimentation experiment under similar conditions. The partial specific volume of 0.754 $cm^3\ g^{-1}$ calculated from the amino acid composition was used for analysis of the association equilibria using the XL-A data analysis software (version 4.01) supplied by Beckman.

Determination of the equilibrium unfolding temperature (t_m)

To determine the equilibrium constant at various temperatures, the PCP-0SH sample at pH 2.3 was filled in the DSC cell and heated at a scan-rate of 90 deg. C/hour to 76 °C to allow complete unfolding. Heating was followed by immediate cooling to various temperatures (28-57 °C) where the sample was left for a sufficient time (6-48 hours depending upon the temperature of incubation) to allow it to reach equilibrium in the DSC cell. Thereafter, it was immediately brought to 30 °C and reheated to 75 °C at a scan-rate of 90 deg. C/hour. The highest available scan-rate was used to minimize the extent of refolding during the temperature scanning period. The enthalpy of unfolding at the second heating (ΔH_2) was divided by the enthalpy of unfolding at the first heating (ΔH_1) to determine the fraction of recovery of the native species and was plotted as a function of temperature of incubation. It was assumed that the native state population should be proportional to the calorimetric enthalpy.

Using a two state denaturation equation as described earlier:[59,60]

$$Y_o = \frac{[Y_N + Y_D \exp(-1/R(\Delta H_m(1/T - 1/T_m) - \Delta C_p(T_m/T - 1 + \ln(T/T_m))))]}{[1 + \exp(-1/R(\Delta H_m(1/T - 1/T_m) - \Delta C_p(T_m/T - 1 + \ln(T/T_m))))]} \quad (13)$$

where Y_o is the observed signal ($\Delta H_2/\Delta H_1$) at any temperature T, Y_N and Y_D are the signals for the pure native and the pure denatured species, respectively; and ΔH_m and t_m are the enthalpy and midpoint of unfolding, respectively; a non-linear least-square fitting was carried out to fit the denaturation data ($\Delta H_2/\Delta H_1$ *versus* temperature) to evaluate the thermodynamic parameters ΔH_m, ΔC_p and t_m.

Determination of the rate of refolding (k_f)

Using time-resolved DSC progress curves

The PCP-0SH at pH 2.3 was heat-denatured at 70 °C for ten minutes and then transferred immediately to various waterbaths pre-thermostated at 4, 18, 25, and 32 °C. The sample aliquots were taken at various time intervals and filled into DSC cells to measure the unfolding curve. The enthalpy of unfolding was evaluated, and the progress curves for refolding were generated as a function of time (enthalpy *versus* time). These progress curves were analyzed by the least-squares method to determine the rate constant using the equation:

$$Y(t) = Y_o + \Sigma A_i e^{-k_i t} \quad (14)$$

where Y is the signal at any time (t), Y_o is the signal value when no further change is observed, k_i is the apparent rate constant, and A_i is the total amplitude of the ith kinetic phase.

From the time-resolved CD spectroscopic progress curves

The refolding of PCP-0SH after heat denaturation at 70 °C for ten minutes at pH 2.3 was followed by the changes in peptidyl and aromatic CD at various temperatures. The dead time was approximately two to four minutes before the data collection started. The CD measurements were carried out using quartz cuvettes with light path-length of 1 mm (1.61 mg/ml of protein concentration) and 10 mm (1.81 mg/ml) at 220 nm and 280 nm, respectively, on a JASCO-J-720 spectropolarimeter equipped with an NEC PC. The temperature of the cuvette holder was controlled by a circulating water-bath (Haake F3, Germany) and monitored continuously by dipping a thermal sensor into the water slot in the cuvette holder. The progress curves were analyzed using equation (14).

Acknowledgements

This work was supported, in part, by a Fellowship from the Japan Society for the Promotion of Science for Foreign Researchers (J.K.K) and a Grant-in-Aid for special project research from the Ministry of Education, Science and Culture of Japan (K.Y.).

References

1. Jaenicke, R., Schurig, H., Beaucamp, N. & Ostendorp, R. (1996). Structure and stability of hyperstable proteins: glycolytic enzymes from hyperthermophilic bacterium *Thermotoga maritima*. *Advan. Protein Chem.* **48**, 181-269.
2. Henning, M., Darimont, B., Sterner, R., Kirschner, K. & Jansonius, J. N. (1995). 2.0 Å structure of indole-3-glycerolphosphatae synthase from the hyperthermophile *Sulfolobus solfataricus*: possible determinants of protein stability. *Structure*, **3**, 1295-1305.
3. Perl, D., Welker, C., Schindler, T., Schroder, K., Marahiel, M. A., Jaenicke, R. & Schmid, F. X. (1998). Conservation of rapid two-state folding in mesophilic, thermophilic and hyperthermophilic cold shock proteins. *Nature Struct. Biol.* **5**, 229-235.
4. Cavagnero, S., Debe, D. A., Zhou, Z. H., Adams, M. W. & Chan, S. I. (1998). Kinetic role of electrostatic interactions in the unfolding of hyperthermophilic and mesophilic rubredoxins. *Biochemistry*, **37**, 3369-3376.
5. Pothekin, S. A., Ogasahara, K. & Yutani, K. (2000). Transition state of heat denaturation of methionine aminopeptidase from a hyperthermophile. *J. Therm. Anal. Calorim.* **62**, 111-122.
6. Wrba, A., Schweiger, A., Schultes, V., Jaenicke, R. & Zavodsky, P. (1990). Extremely thermostable D-glyceraldehyde-3-phosphate dehydrogenase from the eubacterium *Thermotoga maritima*. *Biochemistry*, **29**, 7584-7592.

7. Klump, H., Di Ruggiero, J., Kessel, M., Park, J. B., Adams, M. W. & Robb, F. T. (1992). Glutamate dehydrogenase from the hyperthermophile *Pyrococcus furiosus*. Thermal denaturation and activation. *J. Biol. Chem.* **267**, 22681-22685.
8. Laderman, K. A., Davis, B. R., Krutzsch, H. C., Lewis, M. S., Griko, Y. V., Privalov, P. L. & Anfinsen, C. B. (1993). The purification and characterization of an extremely thermostable α-amylase from the hyperthermophilic archaebacterium *Pyrococcus furiosus*. *J. Biol. Chem.* **268**, 24394-24401.
9. McAfee, J. G., Edmondson, S. P., Zegar, I. & Shriver, J. W. (1996). Equilibrium DNA binding of Sac7d protein from the hyperthermophile *Sulfolobus acidocaldarius*: fluorescence and circular dichroism studies. *Biochemistry,* **35**, 4034-4045.
10. DeDecker, B. S., O'Brien, R., Fleming, P. J., Geiger, J. H., Jackson, S. P. & Sigler, P. B. (1996). The crystal structure of a hyperthermophilic archaeal TATA-box binding protein. *J. Mol. Biol.* **264**, 1072-1084.
11. Pfeil, W., Geierich, U., Kleemann, G. R. & Sterner, R. (1997). Ferredoxin from the hyperthermophile *Thermotoga maritima* is stable beyond the boiling point of water. *J. Mol. Biol.* **272**, 591-596.
12. Pappenberger, G., Schurig, H. & Jaenicke, R. (1997). Disruption of an ionic network leads to accelerated thermal denaturation of D-glyceraldehyde-3-phosphate dehydrogenase from the hyperthermophilic bacterium *Thermotoga maritima*. *J. Mol. Biol.* **274**, 676-683.
13. Ogasahara, K., Lapshina, E. A., Sakai, M., Izu, Y., Tsunasawa, S., Kato, I. & Yutani, K. (1998). Electrostatic stabilization in methionine aminopeptidase from hyperthermophile *Pyrococcus furiosus*. *Biochemistry,* **37**, 5939-5946.
14. Nojima, H., Hon-Nami, K., Oshima, T. & Noda, H. (1978). Reversible thermal unfolding of thermostable cytochrome c-552. *J. Mol. Biol.* **122**, 33-42.
15. McCrary, B. S., Edmondson, S. P. & Shriver, J. W. (1996). Hyperthermophile protein folding thermodynamics: differential scanning calorimetry and chemical denaturation of Sac7d. *J. Mol. Biol.* **264**, 784-805.
16. Knapp, S., Karshikoff, A., Berndt, K. D., Christova, P., Atanssov, B. & Ladenstein, R. (1996). Thermal unfolding of the DNA-binding protein Sso7d from the hyperthermophile *Sulfolobus solfataricus*. *J. Mol. Biol.* **264**, 1132-1144.
17. Consalvi, V., Chiaraluce, R., Giangiacomo, L., Scandurra, R., Christova, P., Karshikoff, A. *et al*. (2000). Thermal unfolding and conformational stability of the recombinant domain II of glutamate dehydrogenase from the hyperthermophile *Thermotoga maritima*. *Protein Eng.* **13**, 501-507.
18. Rosengarth, A., Rösgen, J. & Hinz, H. J. (1999). Slow unfolding and refolding kinetics of the mesophilic Rop wild-type protein in the transition range. *Eur. J. Biochem.* **264**, 989-995.
19. Lassalle, M. W., Hinz, H. J., Wenzel, H., Vlassi, M., Kokkinidis, M. & Cesareni, G. (1998). Dimer-to-tetramer transformation: loop excision dramatically alters structure and stability of the ROP four α-helix bundle protein. *J. Mol. Biol.* **279**, 987-1000.
20. Lassalle, M. W. & Hinz, H. J. (1999). Refolding studies on the tetrameric loop deletion mutant RM6 of ROP protein. *Biol. Chem.* **380**, 459-472.
21. Tsunasawa, S., Nakura, S., Tanigawa, T. & Kato, I. (1998). Pyrrolidone carboxyl peptidase from the hyperthermophilic archaeon *Pyrococcus furiosus*: cloning and overexpression in *Escherichia coli* of the gene, and its application to protein sequence analysis. *J. Biochem.* **124**, 778-783.
22. Tanaka, H., Chinami, M., Mizushima, T., Ogasahara, K., Ota, M., Tsukihara, T. & Yutani, K. (2001). X-ray crystalline structures of pyrrolidone carboxyl peptidase from a hyperthermophile, *Pyrococcus furiosus,* and its Cys-free mutant. *J. Biochem.* **130**, 107-118.
23. Ogasahara, K., Khechinashvili, N. N., Nakamura, M., Yoshimoto, T. & Yutani, K. (2001). Thermal stability of pyrrolidone carboxyl peptidases from the hyperthermophilic Archaeon, *Pyrococcus furiosus*. *Eur. J. Biochem.* **268**, 3233-3242.
24. Lepock, J. R., Ritchie, K. P., Kolios, M. C., Rodahl, A. M., Heinz, K. A. & Kruuv, J. (1992). Influence of transition rates and scan rate on kinetic simulations of differential scanning calorimetry profiles of reversible and irreversible protein denaturation. *Biochemistry,* **31**, 12706-12712.
25. Potekhin, S. A. & Kovrigin, E. L. (1998). Folding under inequilibrium conditions as a possible reason for partial irreversibility of irreversibility of heat-denatured proteins: computer simulation study. *Biophys. Chem.* **73**, 241-248.
26. Ogasahara, K., Nakamura, M., Nakura, S., Tsunasawa, S., Kato, I., Yoshimoto, T. & Yutani, K. (1998). The unusually slow unfolding rate causes the high stability of pyrrolidone carboxyl peptidase from a hyperthermophile, *Pyrococcus furiosus*: equilibrium and kinetic studies of guanidine hydrochloride-induced unfolding and refolding. *Biochemistry,* **37**, 17537-17544.
27. Jackson, S. E. (1998). How do small single-domain proteins fold? *Fold. Des.* **3**, R81-R91.
28. Plaza del Pino, I. M., Ibarra-Molero, B. & Sanchez-Ruiz, J. M. (2000). Lower kinetic limit to protein thermal stability: a proposal regarding protein stability *in vivo* and its relation with misfolding diseases. *Proteins: Struct. Funct. Genet.* **40**, 58-70.
29. Jaenicke, R. & Bohm, G. (1998). Stability of proteins in extreme environments. *Curr. Opin. Struct. Biol.* **8**, 738-748.
30. Plaxco, K. W., Simons, K. T. & Baker, D. (1998). Contact order, transition state placement and the refolding rates of single domain proteins. *J. Mol. Biol.* **277**, 985-994.
31. Fersht, A. R., Itzhaki, L. S., ElMasry, N. F., Matthews, J. M. & Otzen, D. E. (1994). Single versus parallel pathways of protein folding and fractional formation of structure in the transition state. *Proc. Natl Acad. Sci. USA,* **91**, 10426-10429.
32. Mines, G. A., Pascher, T., Lee, S. C., Winkler, J. R. & Gray, H. B. (1996). Cytochrome-c folding triggered by electron-transfer. *Chem. Biol.* **3**, 491-497.
33. Burton, R. E., Huang, G. S., Daugherty, M. A., Calderone, T. L. & Oas, T. G. (1997). The energy landscape of a fast-folding protein mapped by Ala → Gly substitutions. *Nature Struct. Biol.* **4,**, 305-310.
34. Plaxco, K. W., Simons, K. T., Ruczinski, I. & Baker, D. (2000). Topology, stability, sequence, and length: defining the determinants of two-state protein folding kinetics. *Biochemistry,* **39**, 11177-11183.
35. Myers, J. K., Pace, C. N. & Scholtz, J. M. (1995). Denaturant m values and heat capacity changes: relation to changes in accessible surface areas of protein unfolding. *Protein Sci.* **4**, 2138-2148.
36. Doig, A. J. & Williams, D. H. (1991). Is the hydrophobic effect stabilizing or destabilizing in proteins?

The contribution of disulphide bonds to protein stability. *J. Mol. Biol.* **217**, 389-398.
37. Privalov, P. L., Tiktopulo, E. I., Yu. Venyaminov, S., Griko, Yu. V., Makhatadze, G. I. & Khechinashvili, N. N. (1989). Heat capacity and conformation of proteins in the denatured state. *J. Mol. Biol.* **205**, 737-750.
38. Beadle, B. M., Baase, W. A., Wilson, D. B., Gilkes, N. R. & Shoichet, B. K. (1999). Comparing the thermodynamic stabilities of a related thermophilic and mesophilic enzyme. *Biochemistry,* **38**, 2570-2576.
39. Dams, T. & Jaenicke, R. (1999). Stability and folding of dihydrofolate reductase from the hyperthermophilic bacterium *Thermotoga maritima*. *Biochemistry,* **38**, 9169-9178.
40. Jaenicke, R. (1991). Protein stability and molecular adaptation to extreme conditions. *Eur. J. Biochem.* **202**, 715-728.
41. Sugita, Y. & Kitao, A. (1998). Dependence of protein stability on the structure of the denatured state: free energy calculations of I56V mutation in human lysozyme. *Biophys. J.* **75**, 2178-2187.
42. Yamagata, Y., Ogasahara, K., Hioki, Y., Lee, S. J., Nakagawa, A., Nakamura, H. *et al*. (2001). Entropic stabilization of the tryptophan synthase α-subunit from a hyperthermophile, *Pyrococcus furiosus*: X-ray analysis and calorimetry. *J. Biol. Chem.* **276**, 11062-11071.
43. Yip, K. S., Britton, K. L., ., Stillman, T. J., Lebbink, J., de Vos, W. M., Robb, F. T. *et al*. (1998). Insights into the molecular basis of thermal stability from the analysis of ion-pair networks in the glutamate dehydrogenase family. *Eur. J. Biochem.* **255**, 336-346.
44. Waldburger, C. D., Schildbach, J. F. & Sauer, R. T. (1995). Are buried salt bridges important for protein stability and conformational specificity? *Nature Struct. Biol.* **2**, 122-128.
45. Hendsch, Z. S., Jonsson, T., Sauer, R. T. & Tidor, B. (1996). Protein stabilization by removal of unsatisfied polar groups: computational approaches and experimental tests. *Biochemistry,* **35**, 7621-7625.
46. Kajander, T., Kahn, P. C., Passila, S. H., Cohen, D. C., Lehtio, L., Adolfsen, W. *et al*. (2000). Buried charged surface in proteins. *Struct. Fold. Des.* **8**, 1203-1214.
47. Haney, P. J., Konisky, J., Koretke, K. K., Luthey-Schulten, Z. & Wolynes, P. G. (1997). Structural basis for thermostability and identification of potential active site residues for adenylate kinases from the archaeal genus Methanococcus. *Proteins: Struct. Funct. Genet.* **28**, 117-130.
48. Haney, P. J., Badger, J. H., Buldak, G. L., Reich, C. I., Woese, C. R. & Olsen, G. J. (1999). Thermal adaptation analyzed by comparison of protein sequences from mesophilic and extremely thermophilic Methanococcus species. *Proc. Natl Acad. Sci. USA,* **96**, 3578-3583.
49. Watanabe, K., Hata, Y., Kizaki, H., Katsube, Y. & Suzuki, Y. (1997). The refined crystal structure of *Bacillus cereus* oligo-1,6-glucosidase at 2.0 Å resolution: structural characterization of proline-substitution sites for protein thermostabilization. *J. Mol. Biol.* **269**, 142-153.
50. Bogin, O., Peretz, M., Hacham, Y., Korkhin, Y., Frolow, F., Kalb(Gilboa), A. J. & Burstein, Y. (1998). Enhanced thermal stability of *Clostridium beijerinckii* alcohol dehydrogenase after strategic substitution of amino acid residues with prolines from the homologous thermophilic *Thermoanaerobacter brockii* alcohol dehydrogenase. *Protein Sci.* **7**, 1156-1163.
51. Kumar, S., Tsai, C. J. & Nussinov, R. (2000). Factors enhancing protein thermostability. *Protein Eng.* **13**, 179-191.
52. Nölting, B. (1999). *Protein Folding Kinetics*, p 4, Springer-Verlag, Berlin.
53. Huang, G. S. & Oas, T. G. (1995). Submillisecond folding of monomeric λ repressor. *Proc. Natl Acad. Sci. USA,* **92**, 6878-6882.
54. Myers, J. K. & Oas, T. G. (2001). Preorganized secondary structure as an important determinant of fast protein folding. *Nature Struct. Biol.* **8**, 552-558.
55. van Nuland, N. A., Chiti, F., Taddei, N., Raugei, G., Ramponi, G. & Dobson, C. M. (1998). Slow folding of muscle acylphosphatase in the absence of intermediates. *J. Mol. Biol.* **283**, 883-891.
56. Parker, M. J., Sessions, R. B., Badcoe, I. G. & Clarke, A. R. (1996). The development of tertiary interactions during the folding of a large protein. *Fold. Des.* **1**, 145-156.
57. Fujita, S. C., Go, N. & Imahori, K. (1979). Melting-profile analysis of thermal stability of thermolysin. A formulation of temperature-scanning kinetics. *Biochemistry,* **18**, 24-28.
58. Lepock, J. R., Rodahl, A. M., Zhang, C., Heynen, M. L., Waters, B. & Cheng, K. H. (1990). Thermal denaturation of the Ca2(+)-ATPase of sarcoplasmic reticulum reveals two thermodynamically independent domains. *Biochemistry,* **29**, 681-689.
59. Kaushik, J. K. & Bhat, R. (1998). Thermal stability of proteins in aqueous polyol solutions: role of surface tension of water in the stabilizing effect of polyols. *J. Phys. Chem. sect. B,* **102**, 7058-7066.
60. Kaushik, J. K. & Bhat, R. (1999). A mechanistic analysis of the increase in the thermal stability of proteins in aqueous carboxyl acid salt solutions. *Protein Sci.* **8**, 222-233.

Edited by C. R. Matthews

(Received 30 July 2001; received in revised form 27 November 2001; accepted 7 December 2001)

http://www.academicpress.com/jmb

Supplementary Material for this paper comprising two Figures is available on IDEAL